



Exact solution of Bardeen black hole in Einstein–Gauss–Bonnet gravity

Amit Kumar^{1,a}, Dharm Veer Singh^{1,b}, Yerlan Myrzakulov^{2,3,c}, Gulmira Yergaliyeva^{2,d}, Sudhaker Upadhyay^{4,5,e} 

¹ Department of Physics, Institute of Applied Sciences and Humanities, GLA University, Mathura, Uttar Pradesh 281406, India

² Department of General and Theoretical Physics, L.N. Gumilyov Eurasian National University, Astana 010008, Kazakhstan

³ Ratbay Myrzakulov Eurasian International Center for Theoretical Physics, Astana 010009, Kazakhstan

⁴ Department of Physics, K.L.S. College, Magadh University, Nawada 805110, India

⁵ School of Physics, Damghan University, P.O. Box 3671641167, Damghan, Iran

Received: 3 September 2023 / Accepted: 20 November 2023

© The Author(s), under exclusive licence to Società Italiana di Fisica and Springer-Verlag GmbH Germany, part of Springer Nature 2023

Abstract We have obtained a new exact regular black hole solution for the EGB gravity coupled with nonlinear electrodynamics in AdS space. The numerical analysis of horizon structure suggests two horizons exist: Cauchy and event. We also study the thermal properties of this black hole, which satisfy the modified first law of thermodynamics. Moreover, we analyze the local and global stability of the black hole. The $P - V$ criticality and phase transition are also discussed. The critical exponents for the present model exactly match the mean field theory.

1 Introduction

General relativity (GR) is not a complete theory of gravity, as this fails to explain many universe concepts. For instance, this fails to explain the concept of dark matter and dark energy from the first principle. In various contexts, the theory of gravitation needs modification, and people have modified it accordingly. Still, there is no complete theory of GR. Lovelock gravity [1–3] is one of the modified theories of gravity, which mainly emphasizes the higher derivative of gravity in higher dimensions. Recently, the latest developments of modified gravity have been reviewed in cosmology [4].

The importance of Lovelock gravity lies in the fact that this is the most general GR theory, which provides conserved second-order equations of motion in D -dimensions. Gauss-Bonnet (GB) or Einstein–Gauss–Bonnet (EGB) gravity is a special kind of Lovelock gravity in higher dimensions, which appears naturally in the low energy effective action of string theory [5, 6].

Recently, a black hole solution in $4D$ AdS GB massive gravity is obtained [7]. However, a black hole solution in $4D$ AdS EGB black hole with Yang-Mills field is found in Ref. [8]. Here, we are interested in obtaining a black hole solution for $5D$ GB massive gravity with nonlinear source term. Sakharov and Gliner [9, 10] proposed that a de Sitter core with the equation of state $P = -\rho$ or $T_{ab} = \Lambda g_{ab}$ is required to get a non-singular solution, which could provide proper discrimination at the final stage of gravitational collapse. Based on this idea, Bardeen [11] gave the first regular black hole and, 30 years later, Ayon-Beato and Gracia find an exact solution coupled to nonlinear electrodynamics [12–15]. Subsequently, there are many regular black hole solutions obtained. Still, most of this solution are based on Bardeen’s proposal [16–32]. The generalization of the regular black hole in EGB gravity [33–37], $4D$ EGB gravity [38–40], massive gravity [41] are given. The rotating counterpart by using the Newman Janis algorithm [42, 43] for rotating black hole was proposed [44–46]. Recently, the EGB gravity is simplified in an inflationary theoretical framework, which solves the problem of gravity waves having speed equal to that of light [47, 48]. The compact objects (stars) [49] and primordial gravitational waves [50] are also studied for GB gravity.

Thermal properties of black holes have been the subject of interest for many years [51–55]. Black holes are not only characterized by temperature or entropy, but they possess phase structures and admit critical phenomena [56]. In fact, phase transition is important in investigating the black hole’s properties in extended space. Hawking and Page have studied the first phase transition between AdS black hole and thermal AdS [57]. Witten analyzed the confinement/deconfinement phase [58], and Chamblin studied the van

Dharm Veer Singh: Visiting Associate at IUCAA Pune, India
Sudhaker Upadhyay: Visiting Associate at IUCAA Pune, India.

^a e-mail: ammiphy007@gmail.com

^b e-mail: veerdsingh@gmail.com

^c e-mail: ymyrzakulov@gmail.com

^d e-mail: gyergaliyeva1171@gmail.com

^e e-mail: sudhakerupadhyay@gmail.com (corresponding author)

der Wall phase transition of charged AdS black hole [59, 60]. The extended thermodynamics of various black holes are studied for different types of black holes [61–70] and the $P - v$ criticality of the FLRW universe are [71, 72]. Thermodynamics of singular solution for the rotating counterpart of Lee-Wick gravity having a point source in a higher-derivative theory is presented in Ref. [73]. Here, we discuss the thermodynamics of 5D EGB black hole solution with a nonlinear source.

The paper is organized as follows. We obtain the EGB Bardeen AdS black hole solution and also give the relevant equations of EGB gravity coupled to nonlinear electrodynamics with the structure and location of the horizons in Sect. 2. The study of the thermodynamical properties of 5D EGB regular massive black holes is the subject of Sect. 3. We end the paper with results and concluding remarks in Sect. 5. We use the metric signature $(-, +, +, +, +)$ with natural units $8\pi G = c = 1$.

2 Black holes solutions in EGB gravity

The action of EGB gravity coupled with dual nonlinear electrodynamics in AdS spacetime is written as

$$S = \frac{1}{2} \int d^5x \sqrt{-g} [R - 2\Lambda + \alpha \mathcal{L}_{GB} - \mathcal{L}(F)], \tag{1}$$

where R is the Ricci scalar, Λ is the cosmological constant, which can be expressed in terms of the Planck length l as $-6/l^2$, α is the GB coupling and $\mathcal{L}_{GB} = R_{\mu\nu\gamma\delta}R^{\mu\nu\gamma\delta} - 4R_{\mu\nu}R^{\mu\nu} + R^2$ is the Lagrangian density of EGB gravity where $R_{\mu\nu}$ and $R_{\mu\nu\lambda\sigma}$ are the Ricci and Riemann tensor, respectively. Here, Lagrangian \mathcal{L} depends on $F = \frac{1}{4}F_{\mu\nu}F^{\mu\nu}$, where $F_{\mu\nu} = \partial_\mu A_\nu - \partial_\nu A_\mu$ is Maxwell field-strength tensor. J_μ is the current vector corresponding to the source. We study the black hole system in terms of the Plebanski tensor $P_{\mu\nu}$ defined formally as $P_{\mu\nu} := 2\frac{\partial\mathcal{L}}{\partial F^{\mu\nu}} = F_{\mu\nu}\mathcal{L}_F$, where $\mathcal{L}_F = \partial\mathcal{L}/\partial F$. The nonlinear electrodynamics of the considered system can be obtained alternatively by using the Legendre transformation [15]: $\mathcal{H} = 2F\mathcal{L}_F - \mathcal{L}$ which depends on an antisymmetric field ($P = \frac{1}{4}P_{\mu\nu}P^{\mu\nu}$) [15, 74]. Thus, the Lagrangian for nonlinear electrodynamics can be expressed as

$$\mathcal{L} = 2P\mathcal{H}_P - \mathcal{H} \quad \text{and} \quad \mathcal{H}_P = \frac{\partial\mathcal{H}}{\partial P}, \tag{2}$$

where electromagnetic field strength is $F_{\mu\nu} = \mathcal{H}_P P_{\mu\nu}$ and $\mathcal{H}(P)$ is the structure function.

Extremizing the action (1) with respect to metric tensor ($g_{\mu\nu}$) and potential (A_μ) lead to the field equations [12, 15]

$$I_{\mu\nu} \equiv G_{\mu\nu} + H_{\mu\nu} + \Lambda g_{\mu\nu} = T_{\mu\nu} = 2(\mathcal{H}_P P_{\mu\lambda} P^\lambda_\nu - \delta_{\mu\nu}(2P\mathcal{H}_P - \mathcal{H})), \tag{3}$$

$$\nabla_\mu P^{\mu\nu} = \frac{1}{\sqrt{-g}} \partial_\mu (\sqrt{-g} P^{\mu\nu}) = 0. \tag{4}$$

Here, only the time component of J^ν is non-trivial and given by a delta function corresponding to the point source.

Here, the Einstein tensor G_{ab} and the Lanczos tensor H_{ab} are given by [34]

$$G_{\mu\nu} = R_{\mu\nu} - \frac{1}{2}g_{\mu\nu}R, \tag{5}$$

$$H_{\mu\nu} = -\frac{\alpha}{2} [8R^{\rho\sigma} R_{\mu\rho\nu\sigma} - 4R_\mu^{\rho\sigma\lambda} R_{\nu\rho\sigma\lambda} - 4RR_{\mu\nu} + 8R_{\mu\lambda}R^\lambda_\nu + g_{\mu\nu}(R_{\mu\nu\gamma\delta}R^{\mu\nu\gamma\delta} - 4R_{\mu\nu}R^{\mu\nu} + R^2)]. \tag{6}$$

The explicit form of \mathcal{H} will appear later. Here, we want to obtain a 5D regular EGB black hole solution in AdS space-time and investigate its properties. For that, we write the static spherically symmetric metric [41]:

$$ds^2 = -f(r)dt^2 + \frac{1}{f(r)}dr^2 + r^2(d\theta^2 + \sin^2\theta d\phi^2 + \sin^2\theta \sin^2\phi d\psi^2), \tag{7}$$

where $f(r)$ is an unknown metric function which depends on variable r . Therefore, we restrict the electric field to be

$$F_{\mu\nu} = E(r)(\delta_\mu^t \delta_\nu^r - \delta_\nu^t \delta_\mu^r). \tag{8}$$

For the spherically symmetric case, the equation (4) can be expressed as

$$\frac{1}{r^2} \frac{\partial}{\partial r} (r^2 F^{\mu\nu} \mathcal{L}_F) = \frac{\partial}{\partial r} (r^2 P^{\mu\nu}) = 0. \tag{9}$$

Now, the term inside the derivative has to be constant [75] (we choose an electric charge e)

$$r^2 P^{\mu\nu} = -e(\delta_\mu^t \delta_\nu^r - \delta_\nu^t \delta_\mu^r) \implies P^{\mu\nu} = -\frac{e}{r^2}(\delta_\mu^t \delta_\nu^r - \delta_\nu^t \delta_\mu^r), \tag{10}$$

and the invariant P is given by $P = -\frac{e^2}{2r^4}$. The specific structure-function $\mathcal{H}(P)$ that depends on the invariant P is given by

$$\mathcal{H}(P) = \frac{3}{2se^4} \left(\frac{\sqrt{-2e^2P}}{1 + \sqrt{-2e^2P}} \right)^{7/3}, \tag{11}$$

where s is the free parameter related to the ADM mass M and charge e by $s = |e|/2M$. The structure-function (11) justifies the reasonable conditions needed for nonlinear electrodynamics, as this goes over to the Maxwell linear electrodynamics, $\mathcal{H}(P) \rightarrow P$ for the weak fields ($P \ll 1$) and also satisfying the weak energy condition, which requires $\mathcal{H} < 0$ and $\mathcal{H}_P > 0$ [13, 21, 22].

With the help of Eqs. (3) and (10), we derive the non-zero components of the energy-momentum tensor as

$$\begin{aligned} T_t^t &= T_r^r = \frac{3e^3 M}{(r^3 + e^3)^{7/3}}, \\ T_\theta^\theta &= T_\phi^\phi = T_\psi^\psi = \frac{2e^3 M(3e^3 - 4r^3)}{(r^3 + e^3)^{10/3}}. \end{aligned} \tag{12}$$

Using the metric ansatz (7), the non-vanishing components of the Einstein field equation become

$$\begin{aligned} I_t^t &= I_r^r = (4\alpha f'(r) - 2r)(f(r) - 1) - r^3 f'(r) = \frac{6Me^3}{(r^3 + e^3)^{7/3}}, \\ I_\theta^\theta &= I_\phi^\phi = I_\psi^\psi = \frac{2rf' + f + \frac{r^2}{2}f'' + 2\alpha(f'' + f'^2 + f'') - 1}{r^2} = \frac{2e^3 M(3e^3 - 4r^3)}{(r^3 + e^3)^{10/3}}, \end{aligned} \tag{13}$$

where single and double prime are the first and second derivatives, with respect to r , respectively. The above equations lead to the metric function

$$f(r) = 1 + \frac{r^2}{4\alpha} \left(1 \pm \sqrt{1 + \frac{8\alpha M}{(r^3 + e^3)^{4/3}} - \frac{8\alpha}{l^2}} \right). \tag{14}$$

Here, one can see that the solution is characterized by the parameter mass, charge and GB coupling constant. Here, we note that there are two branches (+ve and -ve branch) of solution (14). In the $M = 0$ limit, the black hole solution (14) becomes

$$f(r) = 1 + \frac{r^2}{4\alpha} \left(1 \pm \sqrt{1 - \frac{8\alpha}{l^2}} \right). \tag{15}$$

When $\alpha > 0$ then $8\alpha/l^2 \leq 1$, there is no black hole solution beyond this limit. Thus, the action 1 has two solutions with effective cosmological constants $l_{\text{eff}}^2 = \frac{l^2}{4} \left(1 \pm \sqrt{1 - \frac{8\alpha}{l^2}} \right)$. However, for $8\alpha/l^2 = 1$, both the solutions coincide, and therefore, the theory has a unique AdS vacuum.

The studies of the obtained black hole solutions will help to understand the difference between the other black hole solutions [28, 38] of the similar class of EGB gravity.

1. The source of the obtained black hole solution is unique as this is different from the previous solutions [28, 38]. The departure of Lagrangian density from the other sources of black hole solutions is more evident from the order expansion:

$$\mathcal{L}(P) = \frac{3}{2se^4} (-2e^2 P)^{7/3} \left(1 - \frac{7}{3} \sqrt{-2e^2 P} + \frac{70}{9} (\sqrt{-2e^2 P})^2 + O[P^2] \right). \tag{16}$$

2. The black hole solution is the extension of the Bardeen black hole. In the weak field (large r) limit, the black hole does not reduce to Reissner–Nordstrom black hole, whereas the non-Bardeen class black hole smoothly goes over to it. For small r , the black hole solution reduces to

$$f(r) = 1 + \frac{r^2}{4\alpha} \left[1 \pm \sqrt{1 + \frac{8M\alpha}{r^4} + \frac{32M\alpha e^3}{r^7} - \frac{8\alpha}{r^2} + O[e^6]} \right]. \tag{17}$$

The black hole solution (14) reduces to the Boulware–Deser black hole [78], 5D Bardeen black hole [79] and Schwarzschild–Tangherlin black hole in the limit of $e = 0, \alpha \rightarrow 0$ and $e = 0, \alpha \rightarrow 0$, respectively.

When $\alpha < 0$, the solution (14) still becomes AdS if one takes the -ve signature and dS if one takes the +ve signature. From the vacuum case, the solution (14) with both signs seems reasonable, from which we cannot determine which sign in (14) should be adopted. Then, Boulware and Deser showed that the solution with +ve branch is unstable and the solution is asymptotically an AdS Schwarzschild solution with negative gravitational mass, indicating the instability. The solution (14) with -ve branch is stable and the solution is asymptotically a Schwarzschild solution. This indicates that the +ve branch is of less physical interest. Henceforth, we adopt the negative branch of the solution for further analysis.

This solution behaves at large ($r \rightarrow \infty$) and small ($r \rightarrow 0$) distance as following:

$$\begin{aligned} f(r) &= 1 - \frac{M}{r^2}, & r &\rightarrow \infty \\ f(r) &= 1 - \Lambda_{\text{eff}} r^2, & r &\rightarrow 0 \end{aligned} \tag{18}$$

Table 1 Radius of inner and outer horizons and $\delta = r_+ - r_-$ for different values of charge e

$\alpha = 0.1$				$\alpha = 0.2$			
e	r_-	r_+	δ	e	r_-	r_+	δ
0.493 (e_c)	0.624	0.624	0	0.373 (e_c)	0.566	0.566	0
0.40	0.37	0.81	0.44	0.25	0.27	0.74	0.47
0.45	0.45	0.76	0.31	0.25	0.35	0.71	0.36

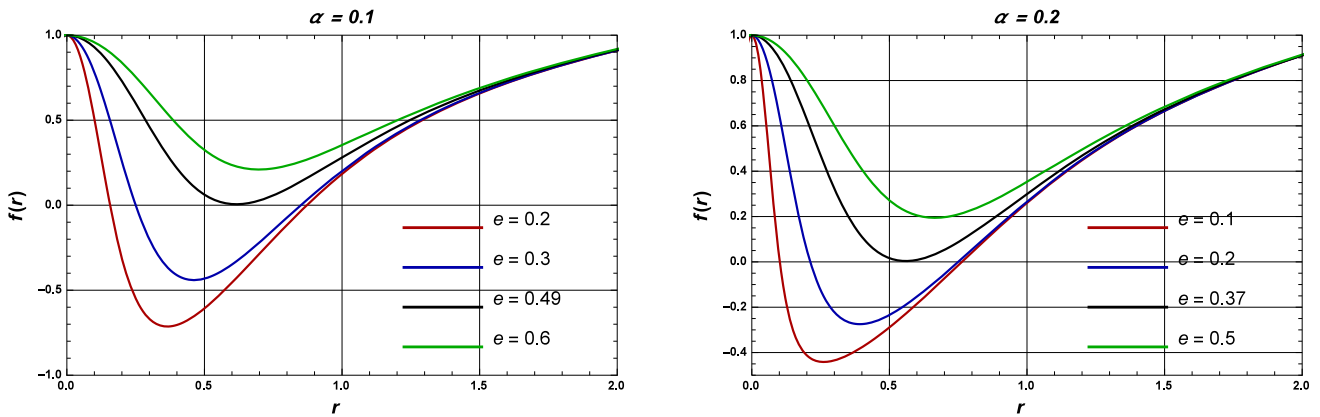


Fig. 1 $f(r)$ vs r corresponding to GB parameter $\alpha = 0.1$ (left) and $\alpha = 0.2$ (right) for different values of charge e

where $\Lambda_{\text{eff}} = \left(1 - \sqrt{1 + 8M\alpha/e^4 - 8\alpha/l^2}\right)/4\alpha$. This implies that the EGB Bardeen AdS black hole solution has a central de Sitter core.

The numerical analysis of horizon condition imparts that there exists non-zero α and e for which metric function $f(r)$ is minimum. However, the horizon condition of metric admits two possible roots for horizon radius r_- and r_+ that correspond to the Cauchy and event horizon, respectively.

We tabulated the numerical values of the inner and outer horizons corresponding to various parameter in Table 1.

The metric function with respect to horizon radius is depicted in Fig. 1.

From Fig. 1 and Table 1, one can see that for a critical value of charge (say e_c) the minimum of metric function is zero (black line curve) and there exists a degenerate horizon. However, for $e < e_c$ the black hole has two horizons r_{\pm} correspond to the non-extremal black hole and for $e > e_c$ there is no horizon, i.e., no black holes. It is noticed that the size of the black hole decreases with the increase in charge and decrease in the GB coupling. This means that the effect of charge and GB coupling are opposite to each other. We can also see that the radius of the event horizon increases with the e and decreases with the α .

The obtained black hole solution is singular if curvature invariants (Ricci scalar R , Ricci square $R_{\mu\nu}R^{\mu\nu}$ and Kretschmann scalar $R_{\mu\nu\lambda\sigma}R^{\mu\nu\lambda\sigma}$) diverge and is regular if curvature invariants converge. Here, for this system, the curvature invariants are calculated by

$$\begin{aligned}
 \lim_{r \rightarrow 0} R &= -\frac{5}{\alpha} + \frac{5}{\alpha} \sqrt{1 + \frac{8M\alpha}{e^4} - \frac{8\alpha}{l^2}}, \\
 \lim_{r \rightarrow 0} R_{\mu\nu}R^{\mu\nu} &= \frac{10}{\alpha^2} + \frac{40}{e^4\alpha} - \frac{10}{\alpha^2} \sqrt{1 + \frac{8M\alpha}{e^4} - \frac{8\alpha}{l^2}}, \\
 \lim_{r \rightarrow 0} R_{\mu\nu\lambda\sigma}R^{\mu\nu\lambda\sigma} &= \frac{5}{\alpha^2} + \frac{20}{e^4\alpha} - \frac{5}{\alpha^2} \sqrt{1 + \frac{8M\alpha}{e^4} - \frac{8\alpha}{l^2}}.
 \end{aligned}
 \tag{19}$$

Here, we find that for $M \neq 0$, the invariants are well-behaved everywhere including the origin. Thus, the EGB Bardeen AdS black hole is a regular (non-singular) black hole.

The obtained black hole solution is regular black holes with a de Sitter core at the Cauchy horizon, $r_0 = r_-$, which is a null surface. The interior region, $r < r_0 = r_-$, is uncharged, satisfying a de Sitter equation of state, where r_0 denotes the surface boundary.

Let us now discuss the features of the three different regions of this regular black hole:

- (I) In the region, $r < r_0 = r_- = R$, the region is uncharged.
- (II) In the region, $r = r_0 = r_- = R$, one has an electrically charged but massless layer.
- (iii) The region, $r > r_0 = r_- = R$, is the Reissner–Nordström like vacuum.

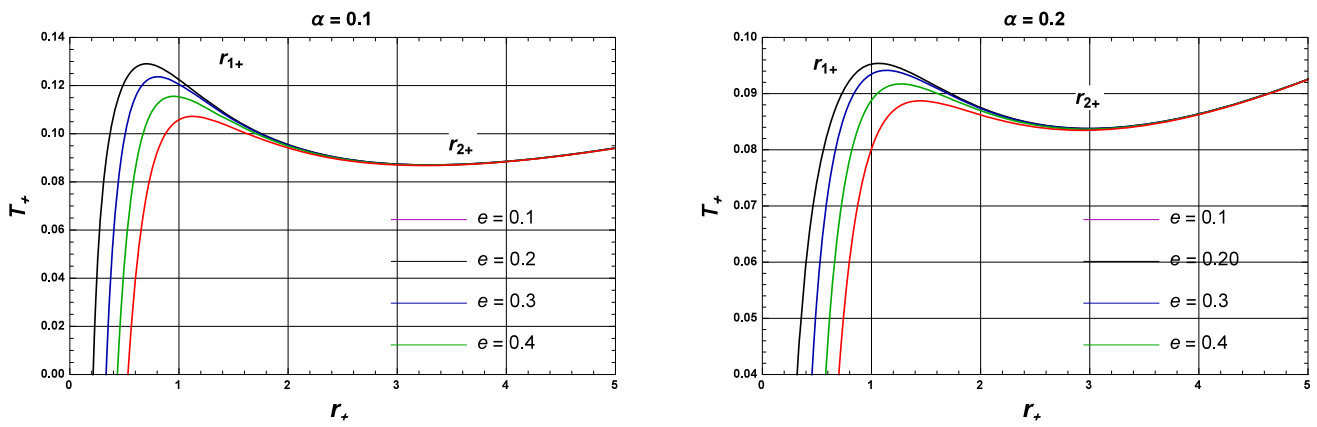


Fig. 2 The plot of temperature Vs. r_+ with different value of electric charge for $\alpha = 0.1$ and $\alpha = 0.2$ with fixed value of e

Table 2 The maximum Hawking temperature (T_+^{Max}) at critical radius (r_c) for different values of charge (e)

	$\alpha = 0.1$					$\alpha = 0.2$				
e	0	0.40	0.45	0.493	0.55	0	0.25	0.30	0.373	0.45
r_c	0.63	0.104	0.108	1.11	1.19	0.897	0.996	1.088	1.36	1.39
T_+^{Max}	0.092	0.097	0.090	0.087	0.082	0.088	0.095	0.0812	0.0786	0.0743

3 Brief comparison with other similar solutions

Recently, in Ref. [76], a black hole solution for 4D EGB gravity with different nonlinear source is discussed and it is shown there that in the large asymptotic limit, the negative branch of the solution which corresponds to Schwarzschild AdS black hole, whereas the positive branch is not physical as it corresponds to the negative mass. However, in vanishing GB parameter, the solution corresponds to Hayward Ads black holes.

In another work [77], a regularized 4D EGB gravity coupled to the different nonlinear electrodynamics is studied and this black hole undergoes a phase transition twice. However, the Hayward and Born–Infeld EGB black holes undergo phase transition only once.

4 Thermodynamics

In this section, we derive thermodynamical quantities of EGB Bardeen AdS black holes solution satisfying the first law of thermodynamics. The mass of the black hole on the horizon is calculated by

$$M_+ = (e^3 + r_+^3)^{\frac{4}{3}} \left(\frac{r_+^2 + 2\alpha}{r_+^4} + \frac{1}{l^2} \right). \tag{20}$$

Using the standard definition, the Hawking temperature corresponding to the given black hole solution is given by

$$T_+ = \frac{f'(r)}{4\pi} \Big|_{r=r_+} = \frac{1}{4\pi r_+(e^3 + r_+^3)(r_+^2 + 4\alpha)} \left[\frac{2r_+^7}{l^2} + 2r_+^5 - 2e^3(r_+^2 + 4\alpha) \right]. \tag{21}$$

From this expression, it is evident that the temperature of the EGB Bardeen AdS black hole is more general than that of EGB black hole [78], Bardeen black hole [79] and Schwarzschild–Tangherilini black hole as the corresponding values of temperature can be achieved by just taking the limiting value of $e = 0$, $\alpha = 0$ and $\alpha = e = 0$, respectively.

To study the nature of temperature corresponding to different parameters, we plot temperature concerning r_+ for different e and α in Fig. 2. From the diagram, we see that the temperature takes a maximum value (T_+^{Max}) corresponding to the minimum metric function.

The numerical values of maximum temperature (T_+^{Max}) corresponding to e and α are tabulated in Table 2. It is obvious from this table that a Hawking temperature takes maximum values at the critical horizon radius. In the extremum limit, (where the Cauchy and event horizons coincide) the temperature vanishes.

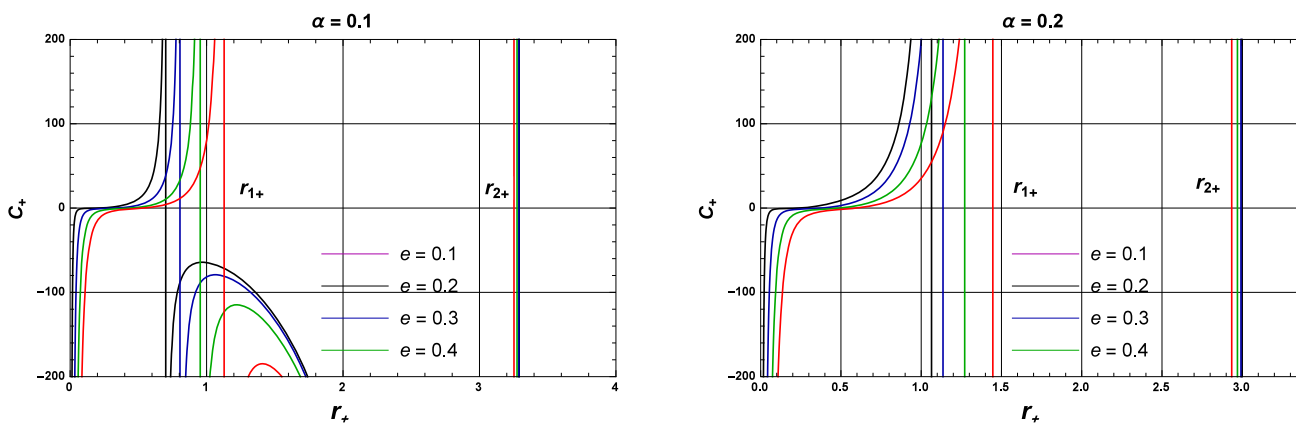


Fig. 3 The plot of heat capacity C_+ Vs. r_+ with different value of electric charge for $\alpha = 0.1$ and $\alpha = 0.2$ with fixed value of e

The first law of black hole thermodynamics follows

$$dM_+ = T_+dS_+ + \Phi de, \tag{22}$$

where Φ is the electric potential corresponding to the electric charge e . Now, we calculate the entropy for the obtained black hole solution (14)

$$S_+ = \int T_+^{-1}dM_+ = \int \frac{1}{T_+} \frac{\partial M_+}{\partial r_+} dr_+ = \frac{4\pi r_+^3}{3} \left[1 + \frac{12\alpha}{r_+^2} - \frac{e^4}{r_+^6}(3r_+^2 + 4\alpha) \right]. \tag{23}$$

Here, we note that the two additional terms in Eq. (23) extend the entropy and the usual area-law $S = \frac{A}{4}$ is no longer valid. In the absence of charge e , the above entropy (23) matches exactly to entropy of EGB black hole [78].

It is well-known that entropy of the regular black hole does not obey the area-law [16, 17, 24, 26, 82] because the energy-momentum tensor already includes the mass of the black hole. To remove the discrepancy, Ma and Zhao proposed the corrected form of the first-law of black hole thermodynamics for regular black holes [80] by introducing an extra factor. The modified first-law thermodynamics [30, 80, 81] reads

$$\xi(M_+, r_+)dM = T_+ dS + \Phi de, \tag{24}$$

where $\xi(M_+, r_+)$ is given by

$$\xi(M_+, r_+) = 1 + 4\pi \int_{r_+}^{\infty} r_+^2 \frac{\partial T_+}{\partial M} dr_+ = \frac{r_+^4}{(r_+^3 + e^3)^{4/3}}. \tag{25}$$

One can easily check that with this value of $\xi(M_+, r_+)$ the entropy of the modified first-law of thermodynamics follows the area-law.

5 Local and global stability

The local and global stability of the thermodynamical system can be emphasized by studying the heat capacity (C_+) and Gibbs free energy (G_+) of the system. For instance, the thermodynamic system remains stable when $C_+ > 0$ or $G_+ < 0$ and unstable when $C_+ < 0$ or $G_+ > 0$. The heat capacity of the thermal system is defined by

$$C_+ = \frac{\partial M_+}{\partial T_+} = \left(\frac{\partial M_+}{\partial r_+} \right) \left(\frac{\partial r_+}{\partial T_+} \right). \tag{26}$$

Substituting the values of mass (20) and temperature (21) into (26), the heat capacity for the Bardeen black hole in EGB gravity has the following expression:

$$C_+ = \frac{4\pi\beta^2[r_+^5(l^2 + 2r_+^2) - e^2l^2\beta]}{r_+^3[e^6l^2\beta^2 + r_+^8(-l^2\beta_1^2 + 2r_+^2\beta_2) + e^3(8r_+^7\beta_3 + l^2(6r_+^5\beta_4 + 64r_+^3\alpha^2))]}, \tag{27}$$

where $\beta = r_+^2 + 4\alpha$, $\beta_1 = r_+^2 - 4\alpha$, $\beta_2 = r_+^2 + 6\alpha$ and $\beta_3 = r_+^2 + 8\alpha$.

The heat capacity with respect to r_+ are plotted in Fig. 3 for different values of e and α which suggests that the heat capacity is divergent at the $r_+ = 1$ and $r_+ = 3.2$ for $\alpha = 0.1$, however, at $r_+ = 1.5$ and $r_+ = 3.0$ for $\alpha = 0.2$ where corresponding temperature has local maxima and local minima. From Fig. 3, we can see clearly that the black hole experiences phase transition twice, firstly,

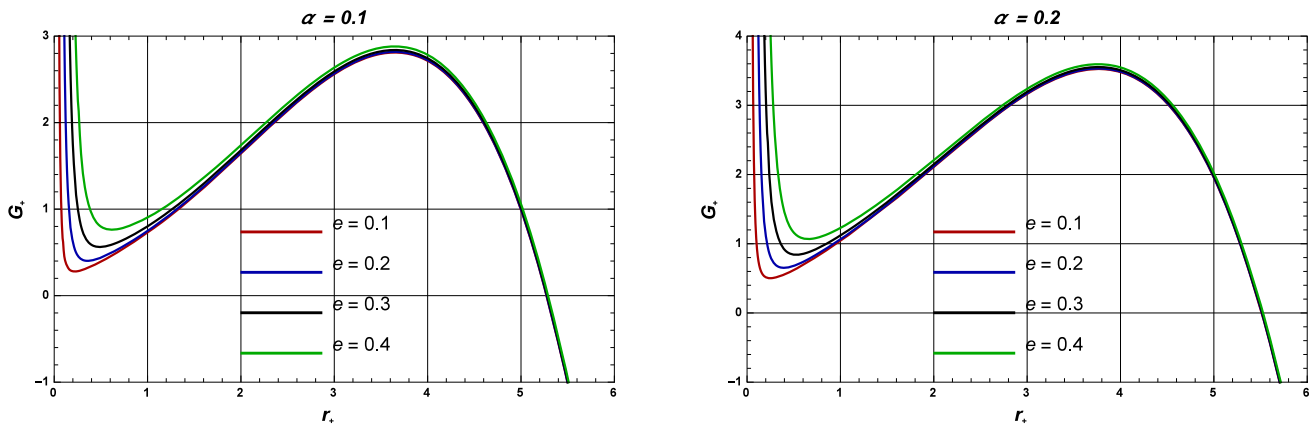


Fig. 4 The plot of Gibbs free energy G_+ Vs. r_+ with different value of electric charge for $\alpha = 0.1$ and $\alpha = 0.2$ with fixed value of e

for smaller stable black holes to larger unstable black holes and, secondly, for smaller unstable black holes to larger stable black holes. The radii r_+ increases with both α and e .

Now, to study the Gibbs free energy, we first estimate using the following expression:

$$G_+ = M_+ - T_+ S_+. \tag{28}$$

Substitute the values of M_+ , T_+ and S_+ , we obtain

$$G_+ = (e^3 + r_+^3)^{4/3} \left(\frac{r_+^2 + 2\alpha}{r_+^4} + \frac{1}{l^2} \right) - \frac{2r_+^2}{3(e^3 + r_+^3)(r_+^2 + 4\alpha)} \left(\frac{r_+^7}{l^2} - (r_+^5 - e^3(r_+^2 + 4\alpha)) \right). \tag{29}$$

At the critical temperature, the Gibbs free energy vanishes. Thus, the critical temperature can be calculated by using $G_+ = 0$ as

$$T_{min} = \frac{3}{4\pi} \frac{(e^3 + r_+^3)^{4/3}}{r_+^3} \left(\frac{r_+^2 + 2\alpha}{r_+^4} + \frac{1}{l^2} \right). \tag{30}$$

The black hole is said to be globally stable when $T_+ > T_C$. However, $T_+ < T_C$ describes the global instability of the black hole.

Generally, the Gibbs free energy demonstrates that black holes with negative values of Gibbs free energy are more thermodynamically stable and unstable for its positive counter parts. To study the nature of Gibbs free energy, we plot (29) in Fig. 4 for different values of e and α . From the figure, we see that the free energy has local minima and local maxima at horizon radii $r_+ = 0.1$ and $r_+ = 3.8$, respectively, where the heat capacity diverges (see Fig. 3) and the temperature attains the extreme values (see Fig. 2). The Hawking–Page first-order phase transition occurs at $r_+ = r_{HP}$, where the free energy turns negative viz., $r_{HP} > r_{b+}$. Thus, the larger black holes, with horizon radii $r_+ = r_{HP}$, are thermodynamically globally stable. However, at very small horizon radii, the Hawking temperature is negative and hence not physical for global stability point of view. This is exactly in accordance with the Hawking–Page phase transition in general relativity. We find that the black hole solution is favored globally with respect to the thermal AdS background solution as $G_+ < 0$ for large r .

6 Phase transition

In this section, the $P - v$ criticality and phase transition for the Bardeen AdS black hole EGB gravity. The cosmological constant is related to the thermodynamic pressure as $\Lambda = -8\pi P$. Thus, the equation of state (EoS) for pressure can be obtained by using Eq. (21) as

$$P_+ = \frac{3}{8\pi r_+^7} (e^3(r_+^2 + 4\alpha) - r_+^5) + \frac{3T_+}{4r_+^6} ((r_+^3 + e^3)(r_+^2 + 4\alpha)). \tag{31}$$

The mass of the black hole has the interpretation of the enthalpy of the thermodynamic system (Fig. 5). Thus, the thermodynamic volume is calculated by

$$V = \left(\frac{\partial M_+}{\partial P_+} \right)_{S_+} = \frac{4\pi}{3} (r_+^3 + e^3)^{4/3}. \tag{32}$$

It is a matter of calculation to obtain the critical radius, critical temperature and critical pressure at the inflection points by using the following relations:

$$\frac{\partial P_+}{\partial r_+} = 0, \quad \frac{\partial^2 P_+}{\partial r_+^2} = 0. \tag{33}$$

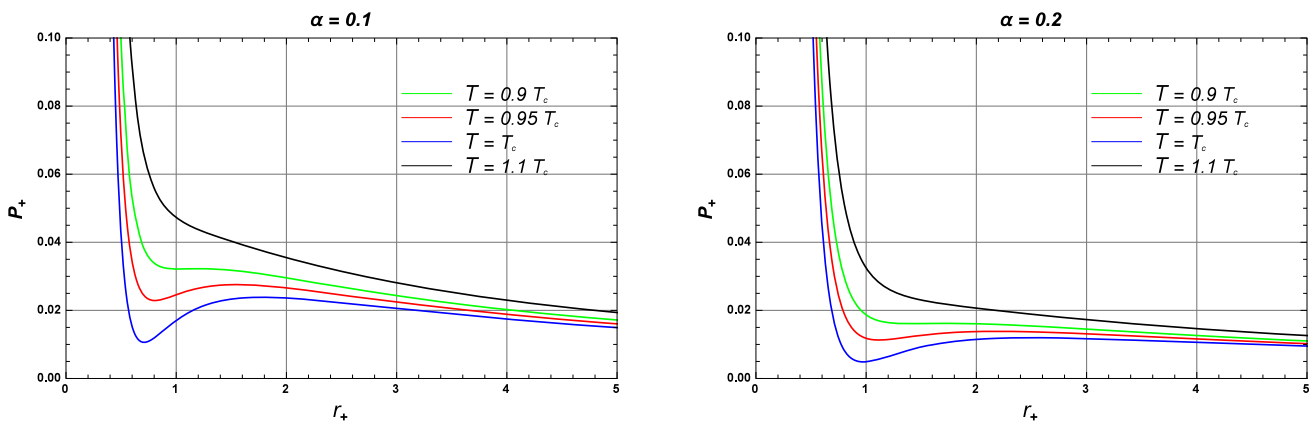


Fig. 5 The plot of pressure Vs. r_+ with different value of temperature T_+ for $\alpha = 0.1$ and $\alpha = 0.2$ with fixed value of e

Table 3 The numerical values of critical radius r_C , critical temperature T_C , critical pressure P_C and $P_C r_C/T_C$ corresponding to various e and fixed $\alpha = 0.1$

e	r_C	T_C	P_C	$P_C r_C/T_C$
0.1	1.112	0.144	0.0327	0.252
0.2	1.204	0.140	0.0302	0.259
0.3	1.362	0.132	0.0260	0.268
0.4	1.552	0.122	0.217	0.276
0.5	1.760	0.112	0.0179	0.281

Table 4 The numerical values of critical radius r_C , critical temperature T_C , critical pressure P_C and $P_C r_C/T_C$ corresponding to various α and fixed e

α	r_C	T_C	P_C	$P_C r_C/T_C$
0.1	1.112	0.144	0.0327	0.252
0.2	1.557	0.102	0.0164	0.250
0.3	1.903	0.0838	0.0110	0.249
0.4	2.195	0.0725	0.0082	0.248
0.5	2.453	0.0649	0.0066	0.247

This relation (33) together with the EoS simplifies to the following expression:

$$r_+^8(r_+^2 - 12\alpha) - 2e^6(5r_+^4 + 54r_+^2\alpha + 16\alpha^2) - 6e^3(3r_+^7 + 40r_+^5\alpha + 112r_+^3\alpha^2) = 0. \tag{34}$$

One cannot solve Eq. (34) analytically. Rather, it is possible to solve it numerically. Here, we calculate the numerical values of critical radius r_C , critical pressure P_C and temperature T_C . The curved portion of the isotherm that is cut off by this straight-line correctly indicates what the allowed states would be if the fluid were homogeneous. However, these homogeneous states are unstable, because there is always another mixed state at the same pressure that possesses a lower Gibbs free energy.

The respective numerical values are presented in Tables 3 and 4 corresponding to the different values of α and e .

It can be seen that the critical radius r_C increases both with e and α . However, the critical temperature T_C and critical pressure P_C decrease with both e and α . Interestingly, in contrast to α case, the universal ratio $P_C r_C/T_C$ increases with e .

To study the phase transition and effects of e and α on the phase transition of this particular black hole, we plot the Gibbs free energy versus temperature as shown in Figs. 6, 7 and 8.

From $G_+ - T_+$ plot 6 with fixed e and α and a certain range of temperature, we observe that there are three kinds of black holes, namely, small ($P < P_C$), intermediate ($P = P_C$) and large black hole ($P > P_C$). Here, the small and large black holes are more stable than the intermediate ones, since the heat capacity is negative (see Fig. 3). We can see that there exists a transition temperature T_* at which a black hole transits from one phase to another phase due to the same free energy. The value of transit temperatures are $T_* = 0.0564$ and $T_* = 0.0358$ for $\alpha = 0.1$ and 0.2, respectively. In Fig. 6, isotherms represent the first-order phase transition at $T_+ < T_*$ and second-order phase transition at $T_+ = T_*$, which is obtained from the free energy diagram (see Fig. 6. At $T_+ < T_*$ the small black hole occurs and at $T_+ > T_*$ large black hole occurs due to small free energy.

In $G_+ - T_+$ plots, the appearance of characteristic swallow tail shape shows the phase transition point. In the left panel of Fig. 6, we see that swallow tail shape occurs at $P < P_C$ for the first-order phase transition and $P = P_C = 0.0327$ for $\alpha = 0.1$ and $P = P_C = 0.0164$ for $\alpha = 0.2$ for the second-order phase transition.

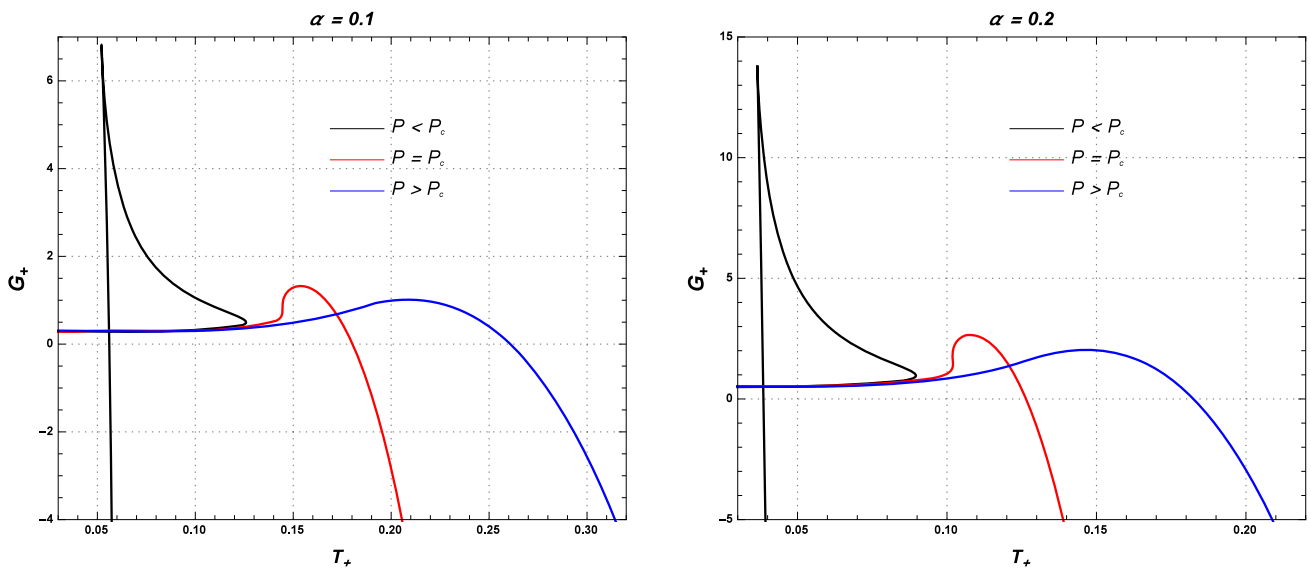


Fig. 6 The plot of Gibbs free energy G_+ versus T_+ with different value of GB coupling with fixed value of e

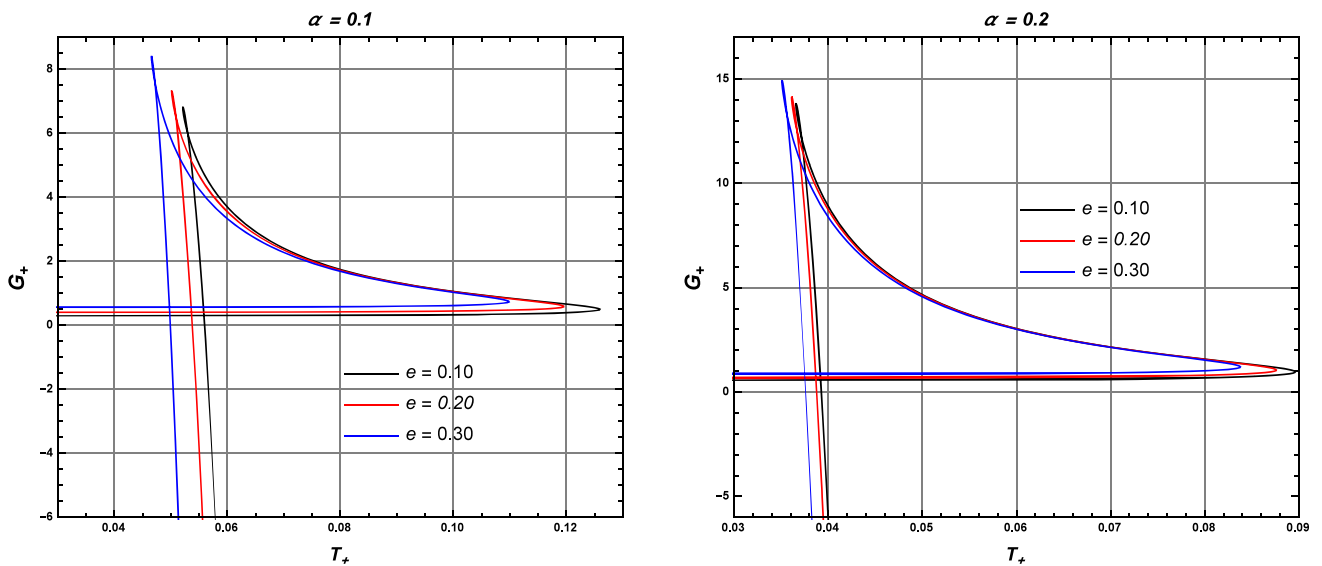


Fig. 7 The plot of Gibbs free energy G_+ Vs. T_+ with different value of e with fixed value of GB coupling

Figures 7 and 8 show the effects of e and α on isobars. The isobars increase with both e and α and the gap between the two sub-critical isobars increases as well. The sub-critical isobar is the regime where the phase transition occurs. It is worth mentioning that the Gibbs free energy in two phases is approximately constant and is less affected by e and α . Interestingly, the universal relation $P_c r_c / T_c$ increases with e and decreases with the GB coupling parameter. This reflects that the effects of electric charge e and GB coupling are opposite to each other.

The black hole are thermodynamically stable state when it has lowest Gibbs free energy. The behavior of Gibbs free energy (G_+) is the function of temperature (T_+) for ($P < P_c$, $P = P_c$) and ($P > P_c$). The plot of Gibbs free energy develops swallow tail structure when ($P > P_c$) which infers the first-order phase transition and the swallow tail structure disappears (first-order phase transition terminates) corresponding to the critical pressure P_c , which infers the second-order phase transition. There is no phase transition, when thermodynamic pressure is larger than the critical pressure P_c . The black hole transits from one phase to another phase due to the same free energy and the corresponding temperature is transition temperature.

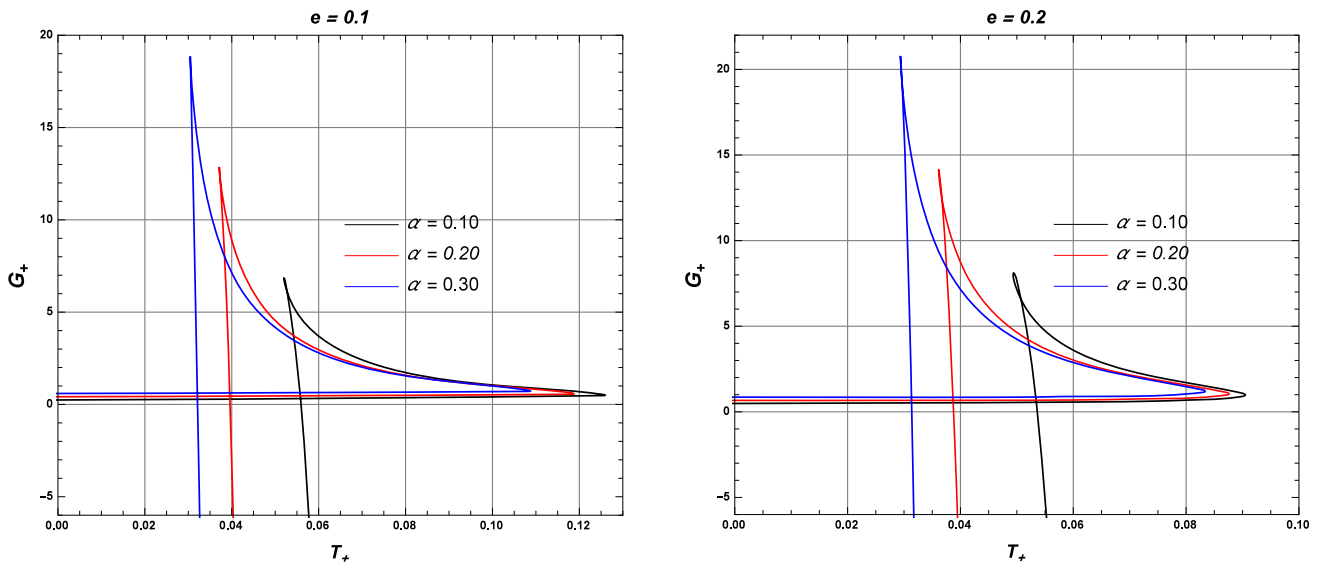


Fig. 8 The plot of Gibbs free energy G_+ Vs. T_+ with different values of GB coupling for fixed value e

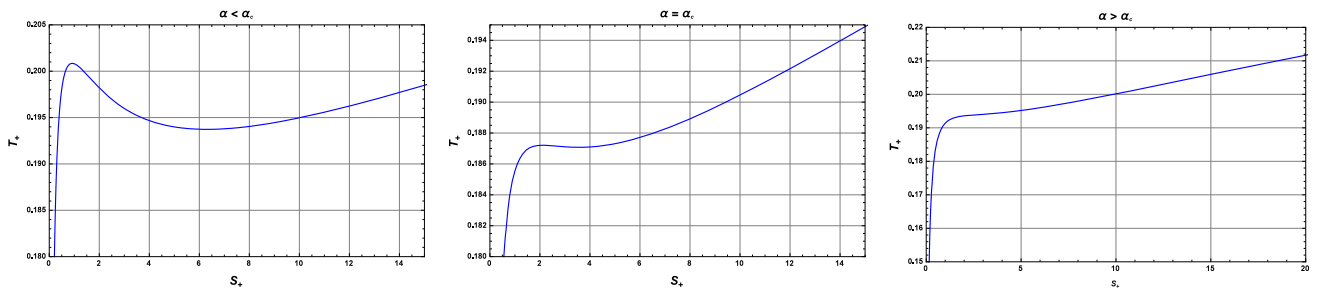


Fig. 9 The plot of T_+ Vs. S_+ . Here we set the parameter $e = 0.1$, $l = 1$ and the critical value of GB parameter (α_c) = 0.0495

7 Phase structure in the framework of AdS/CFT correspondence

In order to study the phase structure from the holography point of view, we first write the Hawking temperature of a given black hole in terms of entropy as follows,

$$T_+ = \frac{8\pi}{(3S_+)^{\frac{1}{3}}(4\pi e^3 + 3S_+)[(3S_+)^{\frac{2}{3}} + 4(4\pi)^{\frac{2}{3}}\alpha]} \left[\frac{1}{l^2} \left(\frac{3S_+}{4\pi} \right)^{\frac{7}{3}} + \left(\frac{3S_+}{4\pi} \right)^{\frac{5}{3}} - e^3 \left(\left(\frac{3S_+}{4\pi} \right)^{\frac{2}{3}} + 4\alpha \right) \right]. \tag{35}$$

Furthermore, to obtain the critical radius, critical temperature and critical the temperature at the inflection points, one can utilize the following relations:

$$\frac{\partial T_+}{\partial S_+} = 0, \quad \frac{\partial^2 T_+}{\partial S_+^2} = 0. \tag{36}$$

In Fig. 9, we plot the scalar isocharges in the $T_+ - S_+$ plane for $\alpha_c = 0.0495$.

According to AdS/CFT correspondence, Ryu and Takayanagi [83, 84] presented an elegant way to calculate the holographic entanglement entropy which is given by the following relation:

$$S_+ = \frac{\text{Area of horizon}}{4G}. \tag{37}$$

The holographic entanglement entropy has the following form [85]:

$$S_+ = \pi \int_0^{\phi_0} r^2 \sin^2 \phi \sqrt{r^2 + \frac{1}{f(r)} \left(\frac{dr}{d\phi} \right)^2} d\phi. \tag{38}$$

Here, we considered $\phi = \phi_0$ as entangling surface and choose the values of ϕ_0 : 0.35, 0.42 and 0.50.

We get the numeric result of $r(\phi)$ with a boundary conditions $r'(0) = 0$ and $r(0) = r_0$. In order to regularize entanglement entropy, we again integrate S in Eq. (38) up to cut-off (which is close to ϕ_0), and subtract the pure AdS entanglement entropy

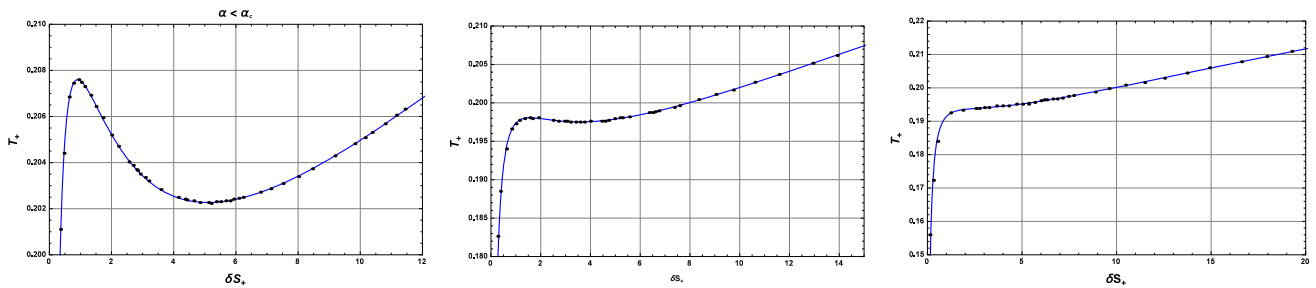


Fig. 10 The plot of T_+ Vs. S_+ . Here we set the parameter $\epsilon = 0.1, l = 1, \phi_0 = 0.35$ and $\phi_c = 0.0495$

(denoted by S'_+) with a same entangling surface ϕ_0 at the boundary. Here, the corresponding regularized entanglement entropy is denoted by $S_+ = S_+ - S'_+$. In Fig. 10, we plot the $T_+ - \delta S_+$ plane for $\phi_0 = 0.35$ as depicted by the dotted curve.

With the help of comparative analysis as given in Fig. 10, we find that the entanglement entropy also presents a Van der Waals-like phase transition.

8 Critical exponents

In this section, we discuss the critical exponents of the fluid behavior of black holes. Since, the Van der Waals-like phase transition is described by the critical exponents α, β, γ and δ near the critical point which shed light on the nature of the heat capacity C_+ , order parameter η , the isothermal compressibility κ_T and the critical isotherm $|P_+ - P_C|_{T_C}$, respectively. These quantities are defined by

$$C_+ = T_+ \frac{\partial S_+}{\partial T_+} \propto |t|^{-\alpha}, \quad \eta = V_l - V_s \propto |t|^\beta, \tag{39}$$

$$\kappa_T = -\frac{1}{V} \frac{\partial V}{\partial P_+} \propto |t|^{-\gamma}, \quad |P_+ - P_C|_{T_C} \propto |V - V_C|^\delta, \tag{40}$$

where $t = \frac{T_+ - T_C}{T_C}$, V_l and V_s are the volumes of a large-sized and the small sized black holes, respectively. Now, we use the following definitions:

$$p = \frac{P_+}{P_C}, \quad \tau = \frac{T_+}{T_C} \quad \text{and} \quad v = \frac{V}{V_C}, \tag{41}$$

Substituting these values in Eq. (31), we get the EoS in terms of dimensionless parameters as

$$p = \frac{1}{\rho_C} \frac{\tau}{v} + 8\alpha \frac{1}{\rho_C V_C^2} \frac{\tau}{v} - \frac{1}{P_C V_C^2} \frac{1}{2\pi v^2} + \frac{1}{V_C^4 P_C} \frac{\alpha + v^2}{\pi v^4}. \tag{42}$$

Let us assume that the law of the critical exponents defined as $p = \frac{1}{\rho_C} \frac{\tau}{v} + h(v)$, where ρ_C is the critical ratio and $h(v)$ is the correction term. Now, expanding this equation near the following critical points:

$$\tau = t + 1, \quad v = (1 + \omega)^{1/z}, \tag{43}$$

and substituting these values of v and ω in Eq. (43), we have

$$\frac{1}{\rho_C} + h(1) = 1, \quad \rho_C h'(1) = 1, \quad \text{and} \quad \rho_C h''(1) = -2. \tag{44}$$

In order to obtain the critical exponents, we expand the EoS near the critical points in the following manner:

$$p = 1 + A_{10}t + A_{11}t\omega + A_{03}\omega^3 + \mathcal{O}(t\omega^2, \omega^4), \tag{45}$$

comparing Eqs. (40) and (37), the coefficients of critical exponents are

$$A_{10} = \frac{1}{\rho_C}, \quad A_{11} = \frac{1}{z\rho_C} \quad \text{and} \quad A_{03} = \frac{1}{z^3} \left(-\frac{h^3(1)}{6} \right). \tag{46}$$

Now, we note that for a phase transition from small to large black holes the pressure and temperature remain constant while volume changes. In this case, the EoS holds and this gives

$$p = 1 + A_{10}t + a_{11}t\omega_s + A_{03}\omega_s^3 = 1 + A_{10}t + A_{11}t\omega_l + A_{03}\omega_l^3. \tag{47}$$

Upon simplification, we have

$$A_{11}t(\omega_l^2 - \omega_s^2) + A_{03}(\omega_l^3 - \omega_s^3) = 0. \tag{48}$$

Moreover, it also follows Maxwell's area law during the phase transition, i.e.,

$$\int_{\omega_s}^{\omega_l} \omega dp = A_{11}t(\omega_l^2 - \omega_s^2) + \frac{3}{2}A_{03}(\omega_l^3 - \omega_s^3) = 0. \quad (49)$$

Solving for the above equations, we obtain a non-trivial solution

$$\omega_l = -\omega_s = \sqrt{\frac{-A_{11}t}{A_{03}}}. \quad (50)$$

With the obtained solution, the order parameter, isothermal compressibility and the shape of critical isotherms read, respectively,

$$\eta = V_C(\omega_l - \omega_s) = 2V_C\omega_l \propto \sqrt{-t}, \quad (51)$$

$$\kappa_T = -\frac{1}{V} \frac{\partial V}{\partial P_+} \Big|_T \propto \frac{1}{P_C} \frac{1}{t}, \quad (52)$$

$$p - 1 \propto -\omega^3, \quad \text{at } t = 0. \quad (53)$$

Consequently, the four critical exponents are $\alpha = 0$, $\beta = \frac{1}{2}$, $\gamma = 1$, $\delta = 3$, which exactly match with the mean field theory.

9 Final remarks and perspectives

We have found a new exact Bardeen AdS black hole in EGB gravity coupled with nonlinear electrodynamics. Our solution interpolates to the Boulware–Deser black hole [78] when $e = 0$, 5D Bardeen black hole when $\alpha \rightarrow 0$ [79] and the Schwarzschild–Tangherlin black hole in the limit of $e = 0$, $\alpha \rightarrow 0$. We have found that the obtained black hole has a central de Sitter core. The horizon structure is discussed numerically as it is not possible to solve it analytically. The black hole has two horizons. The curvature scalars are not singular at the centre which justifies that the obtained solution is regular.

Furthermore, we have studied the thermodynamics of the obtained black holes by computing temperature, entropy, heat capacity and free energy. We have found that this black hole satisfies the modified first law of thermodynamics. The local and global stability are also emphasized by studying the diagram of heat capacity and Gibbs free energy. The phase transition and critical points are also found for this black hole solution. Finally, we found that the critical exponents calculated here are in full agreement with the mean field theory.

Acknowledgements This research has been/was/is funded by the Science Committee of the Ministry of Science and Higher Education of the Republic of Kazakhstan (Grant No. AP09058240). D.V.S. thanks University Grant Commission for the Start Up Grant No. 30-600/2021(BSR)/1630.

Data availability statement No Data is associated with the manuscript.

Declarations

Conflict of interest The authors declare that they have no known competing financial interests or personal relationships that could have appeared to influence the work reported in this paper.

References

1. D. Lovelock, J. Math. Phys. **12**, 498 (1971)
2. D. Lovelock, J. Math. Phys. **13**, 874 (1972)
3. N. Deruelle, L. Farina-Busto, Phys. Rev. D **41**, 3696 (1990)
4. S. Nojiri, S.D. Odintsov, V.K. Oikonomou, Phys. Rept. **692**, 1 (2017)
5. C. Lanczos, Ann. Math. **39**, 842 (1938)
6. B. Zwiebach, Phys. Lett. B **156**, 315 (1985)
7. S. Upadhyay, D.V. Singh, Eur. Phys. J. Plus **137**, 383 (2022)
8. D.V. Singh, B.K. Singh, S. Upadhyay, Ann. Phys. **434**, 168642 (2021)
9. A.D. Sakharov, Sov. Phys. JETP **22**, 241 (1966)
10. E.B. Gliner, Sov. Phys. JETP **22**, 378 (1966)
11. J. Bardeen, in *Proceedings of GR5* (Tiflis, U.S.S.R., 1968)
12. E. Ayon-Beato, A. Garcia, Gen. Rel. Grav. **31**, 629 (1999)
13. E. Ayon-Beato, A. Garcia, Gen. Rel. Grav. **37**, 635 (2005)
14. E. Ayon-Beato, A. Garcia, Phys. Lett. B **493**, 149 (2000)
15. E. Ayon-Beato, A. Garcia, Phys. Rev. Lett. **80**, 5056 (1998)
16. S. Ansoldi. [arXiv:0802.0330](https://arxiv.org/abs/0802.0330) [gr-qc]

17. K.A. Bronnikov, Phys. Rev. D **63**, 044005 (2001)
18. O.B. Zaslavskii, Phys. Rev. D **80**, 064034 (2009)
19. J.P.S. Lemos, V.T. Zanchin, Phys. Rev. D **83**, 124005 (2011)
20. H. Culetu, [arXiv:1408.3334v1](https://arxiv.org/abs/1408.3334v1) [gr-qc]
21. L. Balart, E.C. Vagenas, Phys. Lett. B **730**, 14 (2014)
22. L. Balart, E.C. Vagenas, Phys. Rev. D **90**, 124045 (2014)
23. L. Xiang, Y. Ling, Y.G. Shen, Int. J. Mod. Phys. D **22**, 1342016 (2013)
24. D.V. Singh, N.K. Singh, Ann. Phys. **383**, 600 (2017)
25. D.V. Singh, M.S. Ali, S.G. Ghosh, Int. J. Mod. Phys. D **27**, 1850108 (2018)
26. S. Fernando, Int. J. Mod. Phys. D **26**, 1750071 (2017)
27. D.V. Singh, S.G. Ghosh, S.D. Maharaj, Nucl. Phys. B **981**, 11585 (2022)
28. D.V. Singh, V.K. Bhardwaj, S. Upadhyay, Eur. Phys. J. Plus **137**, 969 (2022)
29. D.V. Singh, A. Shukla, S. Upadhyay, Ann. Phys. **447**, 169157 (2022)
30. D.V. Singh, S.G. Ghosh, S.D. Maharaj, Nucl. Phys. B **981**, 115854 (2022)
31. S.H. Hendi, S. Panahiyan, B. Eslam Panah, Prog. Theor. Exp. Phys. **2015**, 103E01 (2015)
32. S.H. Hendi, A. Sheykhi, S. Panahiyan, B. Eslam Panah, Phys. Rev. D **92**, 064028 (2015)
33. A. Kumar, D.V. Singh, S.G. Ghosh, Ann. Phys. **419**, 168214 (2020)
34. D.V. Singh, S.G. Ghosh, S.D. Maharaj, Ann. Phys. **412**, 168025 (2020)
35. A. Kumar, D.V. Singh, S.G. Ghosh, Eur. Phys. J. C **79**, 275 (2019)
36. S.G. Ghosh, D.V. Singh, S.D. Maharaj, Phys. Rev. D **97**, 104050 (2018)
37. S.G. Ghosh, A. Kumar, D.V. Singh, Phys. Dark Univ. **30**, 100660 (2020)
38. D.V. Singh, R. Kumar, S.G. Ghosh, S.D. Maharaj, Ann. Phys. **424**, 168347 (2021)
39. D.V. Singh, S.G. Ghosh, S.D. Maharaj, Phys. Dark Univ. **30**, 100730 (2020)
40. D.V. Singh, S. Siwach, Phys. Lett. B **408**, 135658 (2020)
41. B.K. Singh, R.P. Singh, D.V. Singh, Eur. Phys. J. Plus **135**, 862 (2020)
42. C. Bambi, L. Modesto, Phys. Lett. B **721**, 329 (2013)
43. S.G. Ghosh, Eur. Phys. J. C **75**, 532 (2015)
44. B. Toshmatov, B. Ahmedov, A. Abdujabbarov, Z. Stuchlik, Phys. Rev. D **89**, 104017 (2014)
45. S.G. Ghosh, S.D. Maharaj, Eur. Phys. J. C **75**, 7 (2015)
46. J.C.S. Neves, A. Saa, Phys. Lett. B **734**, 44 (2014)
47. S.D. Odintsov, V.K. Oikonomou, F.P. Fronimos, Nucl. Phys. B **958**, 115135 (2020)
48. V.K. Oikonomou, Class. Quantum Gravity **38**, 195025 (2021)
49. G.G.L. Nashed, S.D. Odintsov, V.K. Oikonomou, Symmetry **14**, 545 (2022)
50. V.K. Oikonomou, Astropart. Phys. **141**, 102718 (2022)
51. S.H. Hendi, B.E. Panah, S. Panahiyan, J. High Energy Phys. **11**, 157 (2015)
52. S. Upadhyay, Gen. Rel. Grav. **50**, 128 (2018)
53. S. Upadhyay, S.H. Hendi, S. Panahiyan, B.E. Panah, Prog. Theor. Exp. Phys. **2018**, 093E (2018)
54. B. Pourhassan, S. Upadhyay, H. Saadat, H. Farahani, Nucl. Phys. B **928**, 415 (2018)
55. S. Upadhyay, Phys. Lett. B **775**, 130 (2018)
56. D. Kubiznak, R.B. Mann, M. Teo, Class. Quantum Gravity **34**, 063001 (2017)
57. S. Hawking, D. Page, Commun. Math. Phys. **87**, 577 (1983)
58. E. Witten, Adv. Theor. Math. Phys. **2**, 505 (1998)
59. A. Chamblin, R. Emparan, C.V. Johnson, R.C. Myers, Phys. Rev. D **60**, 104026 (1999)
60. A. Chamblin, R. Emparan, C.V. Johnson, R.C. Myers, Phys. Rev. D **60**, 06401 (1999)
61. D. Hansen, D. Kubiznak, R.B. Mann, JHEP **01**, 047 (2017)
62. S.H. Hendi, M. Momennia, Phys. Lett. B **777**, 222 (2018)
63. S.H. Hendi, S. Panahiyan, B. Eslam Panah, Int. J. Mod. Phys. D **25**, 1650010 (2015)
64. R.A. Hennigar, E. Tjoa, R.B. Mann, JHEP **02**, 070 (2017)
65. R.P. Singh, B.K. Singh, B.R.K. Gupta, S. Sachan, Can. J. Phys. **100**, 1 (2022)
66. M.S. Ali, S.G. Ghosh, A. Wang, Phys. Rev. D **108**(4), 044045 (2023)
67. A. Kumar, A. Sood, J.K. Singh, A. Beesham, S.G. Ghosh, Phys. Dark Univ. **40**, 101220 (2023)
68. A. Sood, A. Kumar, J.K. Singh, S.G. Ghosh, Eur. Phys. J. C **82**(3), 227 (2022)
69. H. Abdusattar, Phys. Dark Univ. **40**, 101228 (2023)
70. H. Abdusattar, Eur. Phys. J. C **83**(7), 614 (2023)
71. H. Abdusattar, JHEP **09**, 147 (2023)
72. H. Abdusattar, S.B. Kong, H. Zhang, Y.P. Hu, Phys. Dark Univ. **42**, 101330 (2023)
73. D.V. Singh, S. Upadhyay, M.S. Ali, Int. J. Mod. Phys. A **37**, 2250049 (2022)
74. H. Salazar, A. Garcia, J. Plebanski, J. Math. Phys. **28**, 2171 (1987)
75. M. Born, L. Infeld, Proc. R. Soc. Lond. A **144**, 425 (1934)
76. A. Kumar, S.G. Ghosh, Nucl. Phys. B **987**, 116089 (2023)
77. S.G. Ghosh, D.V. Singh, R. Kumar, S.D. Maharaj, Ann. Phys. **424**, 168347 (2021)
78. D.G. Boulware, S. Deser, Phys. Rev. Lett. **55**, 2656 (1985)
79. M.S. Ali, S.G. Ghosh, Phys. Rev. D **98**, 084025 (2018)
80. M. Ma, R. Zhao, Class. Quantum Gravity **31**, 245014 (2014)
81. R.V. Maluf, J.C.S. Neves, Phys. Rev. D **97**, 104015 (2018)
82. R.M. Wald, Phys. Rev. D **43**, R3427 (1993)
83. S. Ryu, T. Takayanagi, Phys. Rev. Lett. **96**, 181602 (2006)
84. S. Ryu, T. Takayanagi, J. High Energy Phys. **0608**, 045 (2006)
85. H.-L. Li, S.-Z. Yang, X.-T. Zu, Phys. Lett. B **764**, 310 (2017)

Springer Nature or its licensor (e.g. a society or other partner) holds exclusive rights to this article under a publishing agreement with the author(s) or other rightsholder(s); author self-archiving of the accepted manuscript version of this article is solely governed by the terms of such publishing agreement and applicable law.